

A Discrete Element Study of the Earth Pressure Distribution on Cylindrical Shafts

Viet D.H. Tran, Mohamed A. Meguid & Luc E. Chouinard

Department of Civil Engineering and Applied Mechanics— McGill University, Montreal, Quebec, Canada

ABSTRACT

Experimental and numerical studies have been conducted to investigate the earth pressure distribution on cylindrical shafts in soft ground. A small scale laboratory experiment is first described and the measured earth pressure is reported for different conditions of wall movement. The numerical modeling is performed using the discrete element method to allow for the simulation of the large soil displacement and particle rearrangement near the wall. The results of the simulation show a good agreement with the experimental test.

1 INTRODUCTION

Cylindrical structures such as vertical shafts and caissons are widely used in practice. The earth pressure acting on these structures does not generally follow the conventional at-rest or active conditions. Therefore, determining the earth pressure on these structures has received extensive research attention. Experimental and theoretical studies have been conducted by several research groups to understand the mechanics behind the observed lateral pressure distribution along a vertical shaft and calculate stresses in soils surrounding the shaft structure. Several experimental studies have been reported including Walz (1973), Lade et al. (1981), König et al. (1991), Chun & Shin (2006) and Tobar & Meguid (2011) to measure the lateral earth pressure due to the movement of a shaft wall.

Numerical simulation is another approach to understand the mechanics of the problem. One of the challenging tasks to numerically simulate soil-shaft interaction is to account for the large deformations during the shaft wall movement (Dang and Meguid, 2011). While it is difficult to satisfy this requirement using the finite element method, the discrete element method (DEM) provides a promising solution to the problem. The method proposed by Cundall and Strack (1979) has proven to be a versatile approach for the simulation of granular materials. A DEM model is built using a set of discrete particles interacting at contact points, and therefore it is possible to model particle rearrangement and overall behavior of granular soils under large deformations. A DEM study on shaft construction was performed by Herten and Pulsfort (1999). Although the study provided useful results, the circular shaft was assumed to behave as a flat wall. This has led to an inadequate simulation of the arching effect and the stress distribution around the shaft. Furthermore, a quite small segment of the shaft geometry was modeled resulting in the presence of rigid boundaries close to the investigated area which may affect the simulation results. Therefore, there is a need for an improved simulation of the earth pressure acting on cylindrical shafts considering the problem geometry as well as realistic soil properties.

In this paper, an experimental study of a model shaft installed in granular material is presented. The lateral earth pressure acting on the shaft with different wall movements is measured. A DEM simulation of the physical model is then performed. A suitable packing method to generate the soil domain is proposed and a calibration test is conducted to determine the input parameters needed for the simulation. The results of the experimental and numerical studies are then analyzed.

2 EXPERIMENTAL STUDY

An experimental study was performed to investigate the active earth pressure on circular shafts in dry sand. During the experiment, the shaft diameter was uniformly decreased while recording the radial earth pressures at different depths. The experimental setup consisted of an instrumented shaft installed in soil contained within a cylindrical concrete container. Details of the test setup and procedure have been illustrated elsewhere (Tobar and Meguid 2011) and are briefly summarized below:

2.1 Model Shaft

The model shaft consisted of six curved lining segments cut from a steel tube with 101.6 mm in outer diameter and 6.35 mm in thickness. The lining segments were fixed in segment holders which in turn, were attached to hexagonal nuts using steel hinges (see Fig. 1). The nuts could move vertically along an axial rod which could be rotated using a pre-calibrated handle. The shaft was located on a plexiglass plate attached firmly to the base of the container. The initial diameter of the shaft is 150 mm and the length of the shaft is 1025 mm with a soil thickness of 1000 mm.

In order to reduce the diameter of the shaft, the control axial rod is rotated forcing the hexagonal nuts to move vertically; the segment holders and the lining segments are then pulled radially inward. These movements force the diameter of the shaft to decrease uniformly. Two additional segment guide disks were also installed to protect the shaft linings from rotational movement and sliding out of the segment holders.

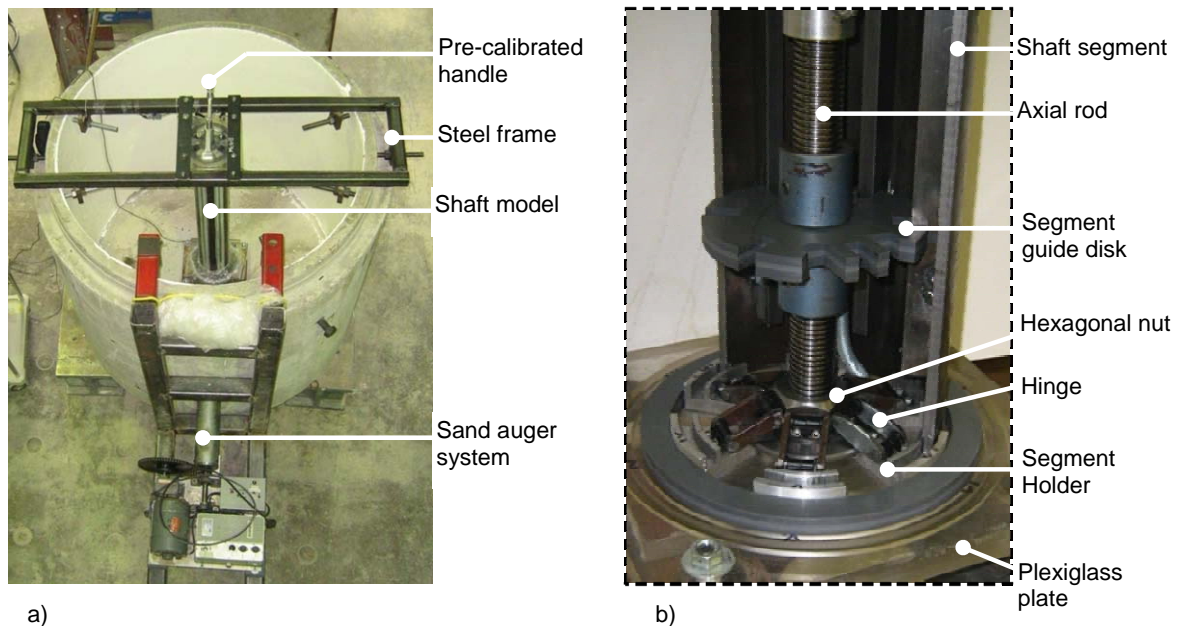


Figure 1. a) An overview of the experimental setup; b) Model shaft during assemblage (from Tobar 2009)

2.2 Concrete Container

A cylindrical concrete tank with inner diameter of 1220 mm provided the axisymmetric condition for the experiment. The tank diameter was chosen to minimize the boundary effects on the behavior of the soil-shaft interaction during the experiment. Previous experimental results of Chun and Shin (2006) and Prater (1977) suggest that failure zone extends from 1 to 3 times the shaft radius. Therefore, negligible soil movement is expected in the present investigation at a radial distance of 240 mm from the outer perimeter of the shaft. The depth of the container is 1070 mm to support the full length of the shaft. The interior side of the container was smoothed and lined with plastic sheets to reduce the soil-wall friction. An overview of the experimental setup and the model shaft is shown in Fig. 1.

2.3 Data Recording Instruments

Load cells and displacement transducers were used to measure the earth pressure and wall movement during the test. Three load cells were installed behind the lining segments at three locations along the shaft which are 840 mm, 490 mm and 240 mm below the sand surface, respectively. The load cells were equipped with sensitive circular areas of one inch diameter in contact with the soil. Two displacement transducers were located near the top and bottom of the shaft lining. All load cells and displacement transducers were connected to a data acquisition system and controlled through a personal computer.

2.4 Testing Procedure

Before every experiment, all instruments were examined and the shaft was adjusted to have an initial diameter of 150 mm. The concrete container was then filled with coarse sand (Granusil silica 2075, Unimin Corp.) through raining process with a target buried depth of one meter from the shaft base. A summary of the sand properties is given in Table 1.

Table 1. Soil properties of the experimental study

Parameter	Value
Specific gravity	2.65
Coefficient of uniformity - C_u	3.6
Coefficient of curvature - C_c	0.82
Void ratio	0.78
Unit weight (kN/m^3)	14.7
Internal friction angle ϕ (deg)	41
Cohesion (kN/m^2)	0

A hopper positioned 1500 mm above the tank was used to spread the sand uniformly over the container. Sand was placed in three layers and once the sand reached slightly over 1-m in height, the pouring process was stopped and extra sand was removed. The sand height was checked using laser sensors to ensure consistent initial conditions for each test. The shaft diameter was then reduced slowly and readings were recorded for each movement increment. A test was

stopped when the reduction in the shaft radius reached 5 mm.

3 DISCRETE ELEMENT SIMULATION

3.1 Discrete Element Method

The discrete element method considers the interaction between distinct particles at their contact points. Different types of particles have been developed including discs, spheres, ellipsoids and clumps. Particles in a sample may have variable sizes to represent the grain size distribution of the real soil. The interaction between particles is regarded as a dynamic process that reaches static equilibrium when the internal forces are balanced. The dynamic behavior is represented by a time-step algorithm using an explicit time-difference scheme. Newton's equations of motion are used to determine particle displacement.

The DEM simulations in this study are conducted using YADE, an open source discrete element code (Kozicki and Donze 2009, Šmilauer et al. 2010). Spherical particles of different sizes are used for this study. The contact law between particles is briefly described below: If two particles A and B with radii r_A and r_B are in contact, the contact penetration depth is defined as:

$$\Delta = r_A + r_B - d_0 \quad [1]$$

where d_0 is the distance between the two centers of particle A and B.

The force vector \vec{F} which represents the interaction between the two particles is decomposed into normal and tangential forces:

$$\vec{F}_N = K_N \vec{\Delta}_N, \quad \vec{F}_T = K_T \delta \vec{\Delta}_T \quad [2a, b]$$

Where \vec{F}_N and \vec{F}_T are the normal and tangential forces; K_N and K_T are the normal and tangential stiffnesses at the contact; $\delta \vec{\Delta}_T$ is the incremental tangential displacement and $\vec{\Delta}_N$ is the normal penetration between the two particles.

K_N and K_T are defined by:

$$K_N = \frac{2Y_A r_A Y_B r_B}{Y_A r_A + Y_B r_B} \quad [3]$$

where "Y" are parameters that control the interaction normal stiffness K_N named "particle material modulus". The interaction tangential stiffness K_T is determined as a given fraction of the computed K_N . The macroscopic

Poisson's ratio is determined by the K_T/K_N ratio while the macroscopic Young's modulus is proportional to K_N and affected by K_T/K_N .

The tangential force \vec{F}_T is limited by a threshold value such that:

$$\vec{F}_T = \frac{\vec{F}_T}{\|\vec{F}_T\|} \|\vec{F}_N\| \tan(\varphi_{micro}) \text{ if } \|\vec{F}_T\| \geq \|\vec{F}_N\| \tan(\varphi_{micro}) \quad [4]$$

where φ_{micro} is the microscopic friction angle.

To represent the rolling behavior between two particles A and B, a rolling angular vector $\vec{\theta}_r$ is used. This vector describes the relative orientation change between the two particles. A resistant moment \vec{M}_r resulting from this change is computed by:

$$\vec{M}_r = \begin{cases} K_r \vec{\theta}_r & \text{if } K_r \|\vec{\theta}_r\| < \|\vec{M}_r\|_{lim} \\ \|\vec{M}_r\|_{lim} \frac{\vec{\theta}_r}{\|\vec{\theta}_r\|} & \text{if } K_r \|\vec{\theta}_r\| \geq \|\vec{M}_r\|_{lim} \end{cases} \quad [5]$$

where:

$$\|\vec{M}_r\|_{lim} = \eta_r \|\vec{F}_N\| \frac{r_A + r_B}{2} \quad [6]$$

K_r is the rolling stiffness of the interaction computed by:

$$K_r = \beta_r \left(\frac{r_A + r_B}{2} \right)^2 K_T \quad [7]$$

where β_r is the rolling resistance coefficient and η_r is a dimensionless coefficient.

To record macroscopic stress components within a representative volume V, the following equation is used:

$$\sigma_{ij} = \frac{1}{V} \sum_{c=1}^{N_c} x^{c,i} f^{c,j} \quad [8]$$

where N_c is the number of contacts within the volume V, $f^{c,j}$ is the contact force vector at contact c, $x^{c,i}$ is the branch vector connecting two contact particles A and B, and indices i and j indicate the Cartesian coordinates.

3.2 DEM Sample Generation

In this study, an appropriate sample generation technique is proposed in order to generate DEM samples for both the calibration test and shaft simulation. Since the sand used in the physical test was generated in layers under gravity, the gravitational approach appears to be a suitable choice in the present study. This method generates anisotropic soil domain which is appropriate to model the lateral earth pressure acting on the shaft.

The gravitational packing technique used in this study is a multi-layer packing method. This packing technique originated from the one proposed by Ladd (1978) for real specimen preparation and is similar to the Multi-layer with Under-compaction Method proposed by Jiang et al. (2003). Modifications are made to simulate the real packing of the sand around the vertical shaft. The packing procedure is described as follow:

The number of layers is first chosen and the volume of particles for each layer is calculated based on the target void ratio of the final soil specimen. To generate the first layer, a set of non-contacting particles is first generated inside a box following a pre-determined particle size distribution until the target volume is reached. The height of the box is chosen to be larger than the target height of the layer to insure that all particles can be generated without overlapping. Gravity is then applied to all particles allowing them to move downward and come in contact with each other. The interparticle friction angle is set to zero. To increase the density of the packing, lateral shaking movement is applied to the box to help small particles move into voids between larger particles. The first layer generation is completed when the system reaches equilibrium. For the second layer, the height of the box is increased and the second "cloud" of non-contacting particles is generated in the area above the existing particles. Gravity and shaking are then applied and the system is allowed to come into equilibrium. The procedure is repeated until the final specimen is formed. The proposed multi-layer approach helps increase the density of the packing while keeping the packing pattern realistic. A packing process of about 200,000 particles using 10 packing layers requires nearly 48 running hours on a personal computer to reach equilibrium which is considered acceptable with respect to DEM simulations.

The behavior of a DEM specimen depends not only on the packing structure but also on the particle size distribution. However, the true replication of grain size is usually restricted by the high computational cost caused by the large number of particles. In this study, particles smaller than D₅ (particle diameter corresponding to 5% passing) are neglected in this study to reduce the computational time. This is appropriate as these particles are assumed to have minor effect on the force chains that transmit stresses within the sample (Cheung 2010, Calvetti 2008).

For the simulation of large scale problems, particle up-scaling is often used to reduce the number of modeled particles. Careful consideration of particle sizes is usually made to keep balance between the computational cost and the scaling effects on the sample responses. In this study, the scale factors (ratio of a numerical particle size

to its real particle size) are chosen as 4 and 25 for the direct shear test and the large scale shaft simulation respectively and will be discussed in following sections. The real particle size distribution used in the analysis is shown in Table 2.

Table 2. Grain size distributions (after removing particles smaller than D₅)

Sieve diameter (mm)	% passing (weight)
0.25	0
0.425	22
0.85	45
1.00	100

3.3 Model Calibration

In order to determine the input parameters for the numerical modeling, calibration is first conducted using the results of direct shear tests. Numerical simulations of direct shear tests are performed and microscopic parameters for the DEM simulation are identified by comparing the numerical results with the physical test data.

The apparatus used for the physical tests consists of a shear box of square cross section (60 mm x 60 mm) split horizontally into two halves. Three different normal stresses, 13.6 kPa, 27.3 kPa and 40.9 kPa were used in this study using vertical loads applied on top of the shear box. The initial sample height was about 25 mm with the height to width ratio of 1: 2.4.

The numerically simulated shear box consists of two parts and each part comprises 5 rigid boundaries: one horizontal boundary and four vertical boundaries (Fig. 2). The numerical shear box has the same dimensions as the actual one to replicate the testing conditions. A specimen is generated using the gravitational method illustrated in the previous section with one packing layer. Using a scale factor of 4, the generated specimen consists of over 14,000 particles with diameters ranging from 1.0 mm to 4.0 mm. After the sample generation is completed, the specimen is subjected to three different vertical stresses of 13.6 kPa, 27.3 kPa and 40.9 kPa.

The calibration is generally a challenging task as the behavior of discrete element samples depends not only on microscopic parameters but also on particle shapes, particle size distribution, contact models and packing technique. While the adopted packing method and particle size distribution are considered realistic, spherical particle shapes and the contact model are somewhat artificial. These assumptions are usually overcome by choosing appropriate input parameters for the simulation.

The most important microscopic parameters that affect the behavior of the direct shear test are the friction angle, the rolling resistance and the stiffnesses. These parameters are varied to match the simulation results with the real test data. Other parameters are identified as follow: particle density is 2650 kg/m³, particle cohesion is zero and the KT/KN ratio is fixed to be 0.25 as suggested by Calvetti (2008).

The rolling resistance coefficient β_r together with the normal and tangential stiffnesses are varied first to match the slope of the curve, the friction angle is then modified to match the peak shear stress. It is observed that the most appropriate combination is a friction angle of 34° , β_r of 0.05, and a particle material modulus of 38 MPa. A summary of the selected parameters is given in Table 3. The normal stress - shear stress relationship is given in Fig. 3. The figure shows a good agreement between the numerical and physical direct shear tests.

Table 3. Particles' properties for DEM simulations

Parameter	Value
Particle density (kg/m^3)	2650
Particle material modulus Y (MPa)	38
Ratio K_T/K_N	0.25
Friction angle ϕ (degrees)	34
β_r	0.05
η_R	1

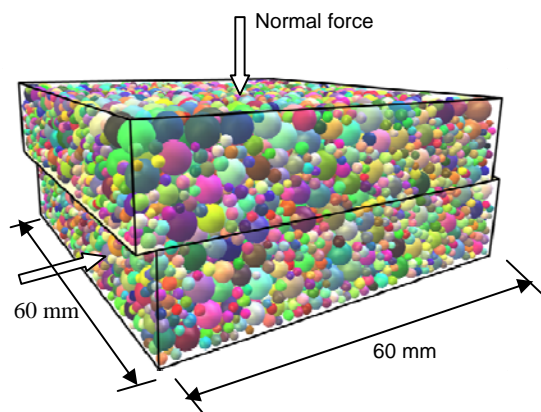


Figure 2. Three-dimensional direct shear sample

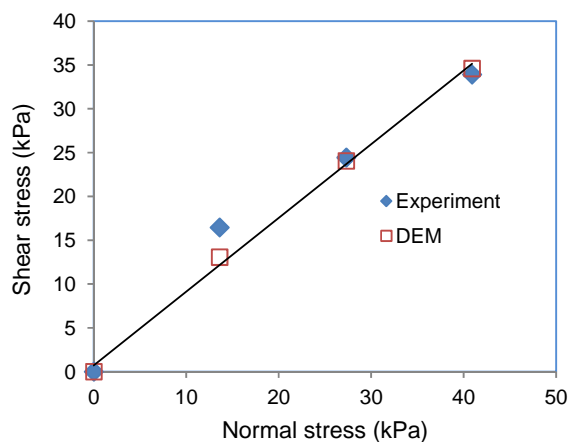


Figure 3. Direct shear test results

3.4 Shaft-Soil Modeling

The vertical shaft is modeled using a cylinder 1.0 m in height and initial diameter of 150 mm that comprises 12 equally distributed segments. Since the modeled problem is axisymmetric, only part of the domain is modeled to reduce the computational cost. In addition, better representation of the experiment can be achieved by simulating one "slice" of the soil domain with a large number of particles while keeping the simulation time acceptable. To capture the problem geometry, a quarter of the problem is modeled in this study. The model consists of a quarter of the shaft and four boundaries including three vertical and one horizontal at the bottom of the container (Fig. 4). Each quarter of the shaft is divided into three segments to capture the curved shaft geometry. The friction angles between particles and the wall boundaries are set to zero and pressures acting on the shaft are recorded at the middle segment to reduce the boundary effects. Similar technique has been used by Weatherley et al. (2011) to model slope collapse and hopper flow problems.

The soil domain is generated using the proposed multi-layer packing technique with 10 layers. Using a scale factor of 25, a total of over 245,000 particles are generated with diameters ranging from 6.25 mm to 25 mm. The average void ratio of the generated soil sample is about 0.85 which is slightly greater than the void ratio of the real sand (0.78). This is attributed to the removal of excess sand to reach the target sample height.

The input parameters for the simulation are then assigned to the particles based on the results of the calibration test. The friction coefficient between the particles and the shaft is assumed to have a value of 0.2 to account for the frictional contact between the shaft and the soil. The diameter of the shaft is incrementally reduced to model the active condition. Lateral earth pressures on the shaft and stresses in the soil domain are recorded at different wall movements using Eq. 8. The simulation process finishes when the reduction in the shaft radius reaches 5 mm.

4 RESULTS AND DISCUSSIONS

Selected experimental results (tests T1, T3 and T4) are reported in this section at three different locations. The measured earth pressure is then compared with the DEM simulation results. The calculated and measured initial earth pressures on the shaft wall are shown in Fig. 5 along with the conventional at-rest condition (K_0 -line where $K_0 = 1 - \sin \phi$). The DEM results were found to be consistent with the measured earth pressure except near the foot of the shaft. This behavior has been observed by other researchers (Herten and Pulsfort 1999, Imamura et al. 1999) and was attributed to the arching effects resulting from the initial compression of the lower sand layers.

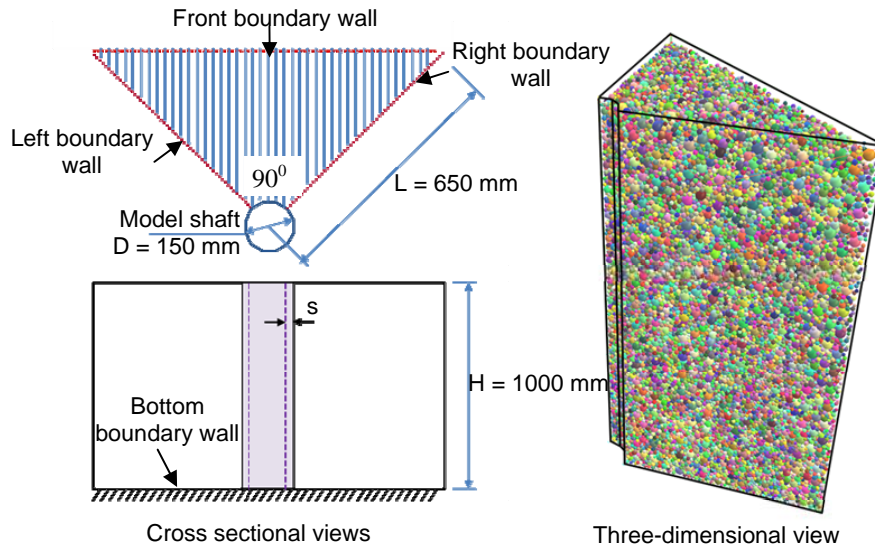


Figure 4. Sectional and 3-D views of the model shaft

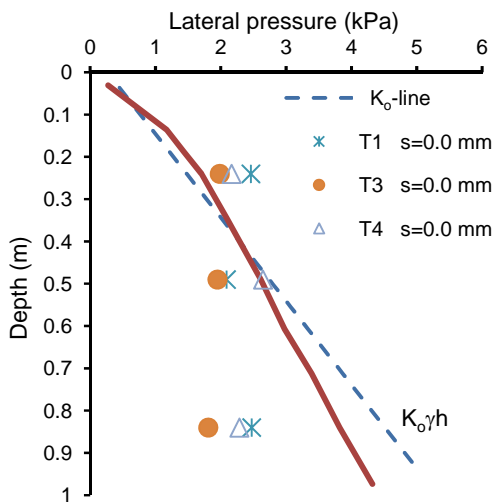


Figure 5. Initial earth pressures on the shaft

Lateral pressures at different locations along the shaft are shown in Figs. 6 to 9. The pressures are plotted versus the wall movement. Both the DEM simulation and the experimental results showed a consistent reduction in lateral pressures as the wall movement increases. The earth pressure became independent of the wall movement when the displacement reached about 3 mm. To study the effects of the wall movement on the active earth pressure, the pressure p at a certain depth is normalized with respect to the initial pressure p_0 . Normalized earth pressures at three depth levels 0.24H, 0.49H and 0.84H for different shaft wall movements are illustrated in Figs. 10, 11 and 12, respectively. It can be seen that the DEM results are in good agreement with the experimental data. For a very small wall movement, a large reduction in lateral earth pressure is observed. At

wall movement of 0.5 mm, the calculated earth pressures decreased from 100% at the initial state to 50% at 0.24H and 0.49H and to 30% at 0.84H. For the same wall movement, the measured earth pressures reached about 65% at 0.24H and 0.49H and about 45% at 0.84H. With further increase in wall movement, the DEM results were found to be identical to the measured values. For movements between 1 mm and 2 mm, the earth pressure decreased to 30% of the initial value at 0.24H and 0.49H and to 18% at 0.84H. Additional movements larger than 3 mm did not cause significant pressure reduction and the lateral pressures became constant when reached approximately 20% of the initial pressure at 0.24H and 0.49H and approximately 10% at 0.84H. It can be concluded that the axisymmetric active earth pressure fully develops when the shaft wall moves about 2 to 3 mm or about 2.5% to 4% of the shaft radius. Furthermore, the most rapid reduction in the earth pressure is observed near the bottom of the shaft.

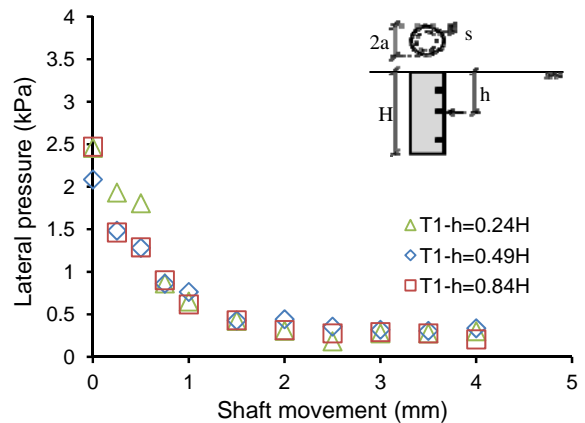


Figure 6. Earth pressures on the shaft at different depths (test T1)

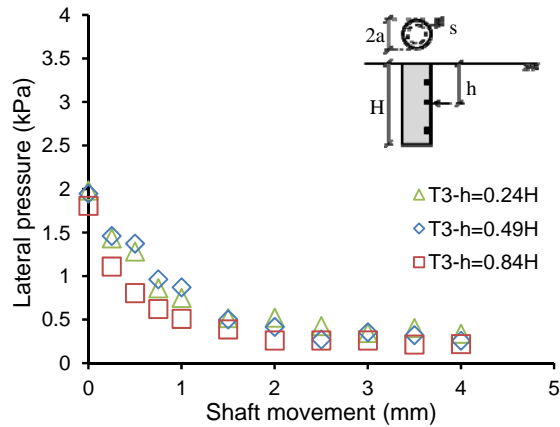


Figure 7. Earth pressures on the shaft at different depths (test T3)

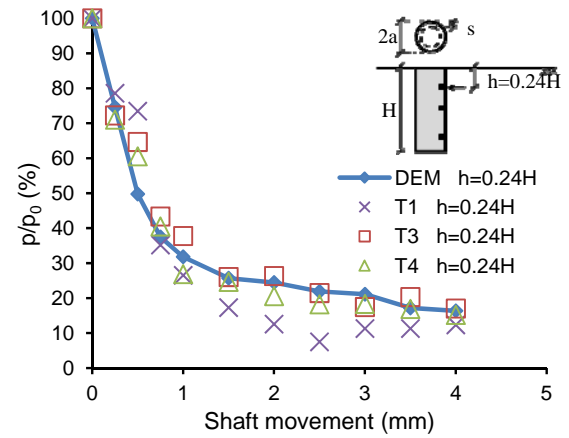


Figure 10. Normalized pressures on the shaft at the depth 0.24H

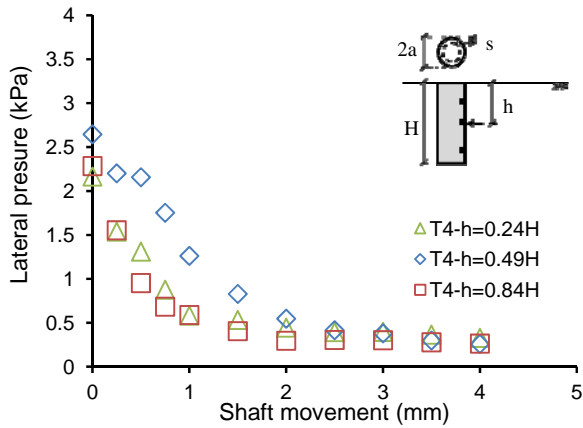


Figure 8. Earth pressures on the shaft at different depths (test T4)

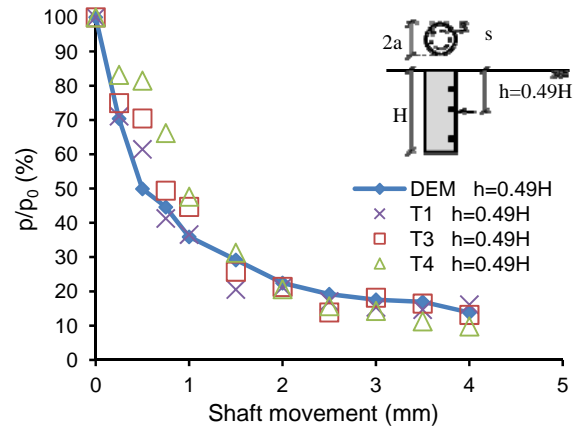


Figure 11. Normalized pressures on the shaft at the depth 0.49H

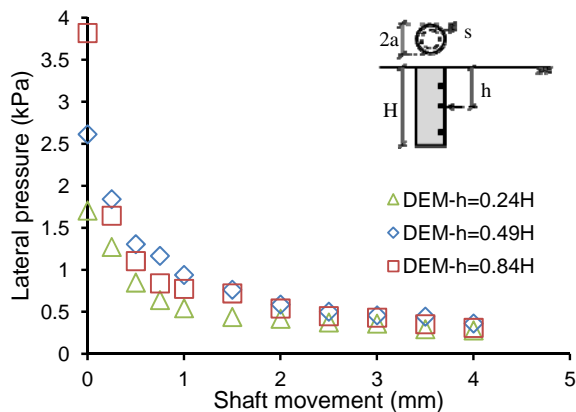


Figure 9. Earth pressures on the shaft at different depths (DEM simulation)

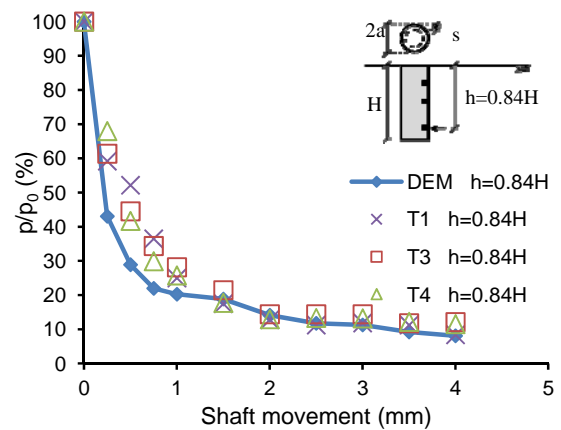


Figure 12. Normalized pressures on the shaft at the depth 0.84H

5 SUMMARY AND CONCLUSIONS

In this paper, an experimental study was performed to investigate the lateral earth pressure acting on a cylindrical shaft. The axisymmetric geometry of the test setup allowed for a proper recording of the earth pressure. A numerical modeling was performed using the DEM. A modified multi-layer gravitational packing method that is able to capture some of the important properties was proposed to generate the soil domain. The particle size distribution of the real sand was considered and a calibration was conducted on the direct shear test to determine input parameters needed for the discrete element analysis. A quarter of the shaft geometry was modeled and the lateral pressures acting on the shaft wall were recorded. The results of the experimental and numerical studies were compared.

The DEM simulation of the vertical shaft agreed well with the experimental data. Based on the experimental and numerical studies, a small shaft movement can lead to a rapid decrease in the earth pressure acting on the shaft. The required shaft movement to reach the full active condition was found to range from 2.5% to 4% of the shaft radius or from 0.2% to 0.3% of the shaft height. At this wall movement, the earth pressure can significantly decrease to a value of 10% of the initial pressure and the lateral pressure becomes uniform with depth.

A good agreement between the numerical and measured results demonstrates the efficiency of the DEM in modeling geotechnical problems involving granular materials and large deformations.

ACKNOWLEDGEMENTS

This research is supported by a research grant from the Natural Sciences and Engineering Research Council of Canada (NSERC). The financial support provided by McGill Engineering Doctoral Award (MEDA) to the first author is greatly appreciated. The authors also wish to acknowledge Tatiana Tobar for her experimental work at McGill University.

REFERENCES

- Calvetti, F. 2008. Discrete modelling of granular materials and geotechnical problems, *European Journal of Environmental and Civil Engineering*, 12: 951-965.
- Cheung, G. 2010. Micromechanics of sand production in oil wells, *Ph.D thesis*, Imperial College London.
- Chun, B., and Shin, Y. 2006. Active earth pressure acting on the cylindrical retaining wall of a shaft, *South Korea Ground and Environmental Engineering Journal*, 7(4): 15-24.
- Cundall, P. A., and Strack O. D. L 1979. A discrete numerical model for granular assemblies, *Géotechnique*, 29(1): 47-65.
- Dang, H.K. and Meguid, M.A. (2011) An efficient finite-discrete element method for quasi-static nonlinear soil-structure interaction problems, *International Journal for Numerical and Analytical Methods in Geomechanics*, (in press).
- Herten, M., and Pulsfort, M. 1999. Determination of spatial earth pressure on circular shaft constructions, *Granular Matter*, 2(1): 1-7.
- Imamura, S., Nomoto, T., Fujii, T., and Hagiwara, T. 1999. Earth pressures acting on a deep shaft and the movements of adjacent ground in sand, In: O. Kusakabe, K. Fujita, and Y. Miyazaki, Eds., *Proceedings of the international symposium on geotechnical aspects of underground construction in soft ground*, Tokyo, Japan: Balkema, Rotterdam, 647-652.
- Jiang, M. J., Konrad, J. M., and Leroueil, S. 2003. An efficient technique for generating homogeneous specimens for DEM studies, *Computers and Geotechnics*, 30 (7): 579–597.
- Konig, D., Guettler, U., and Jessberger, H. L. 1991. Stress redistribution during tunnel and shaft construction, *Proceedings of the International Conference Centrifuge 1991*, Boulder, Colorado, 129-135.
- Kozicki, J., and Donze, V. F. 2009. YADE-OPEN DEM: an open-source software using a discrete element method to simulate granular material, *Engineering Computations*, 26(7): 786 – 805.
- Ladd, R. S. 1978. Preparing test specimens using undercompaction, *Geotechnical Testing Journal*, GTJODJ 1978, 1(1): 16-23.
- Lade, P. V., Jessberger, H. L., Makowski, E., and Jordan, P. 1981. Modeling of deep shafts in centrifuge test, *Proceedings of the International Conference on Soil Mechanics and Foundation Engineering*, Stockholm, Sweden, Vol. 1, pp 683-691.
- Prater, E. G. 1977. Examination of some theories of earth pressure on shaft linings, *Canadian Geotechnical Journal*, 14(1): 91-106.
- Šmilauer, V., Catalano, E., Chareyre, B., Dorofeenko, S., Duriez, J., Gladky, A., Kozicki, J., Modenese, C., Scholtès, L., Sibille, L., Stránský, J., and Thoeni, K. 2010. Yade Documentation, *The Yade Project 2010*. (<http://yade-dem.org/doc/>).
- Tobar, T. 2009. An experimental study of the earth pressure distribution on cylindrical shafts, *Master's thesis*, McGill University.
- Tobar, T., and Meguid, M. A. 2011. Experimental study of the earth pressure distribution on cylindrical shafts, *ASCE Journal of Geotechnical and Geoenvironmental Engineering*, 137(11): 1121-1125.
- Walz, B. 1973. Left bracket apparatus for measuring the three-dimensional active soil pressure on a round model caisson right bracket, *Baummaschine und Bautechnik*, 20(9): 339-344 (in German).
- Weatherley, D., Boros, V., and Hancock, W. 2011. *ESyS - Particle Tutorial and User's Guide Version 2.1*, The University of Queensland.